Journal of Neuroscience Research 53:239–250 (1998)

NADPH-Diaphorase Histochemistry Reveals Heterogeneity in the Distribution of Nitric Oxide Synthase-Expressing Interneurons Between Olfactory Glomeruli in Two Mouse Strains

E. Weruaga, C. Crespo, A. Porteros, J.G. Briñón, R. Arévalo, J. Aijón, and J.R. Alonso*
University of Salamanca, Department of Cell Biology and Pathology, Salamanca, Spain

The expression of nitric oxide synthase (NOS) in the olfactory bulb was compared between two mouse strains, CD-1 and BALB/c, that differ in the connectivity within their olfactory glomeruli, their content of tyrosine hydroxylase, and their response to olfactory deafferentation. Labelled cells were qualitatively and quantitatively analyzed by both immunohistochemistry for NOS and histochemistry for nicotinamide adenine dinucleotide phosphate (NADPH)-diaphorase (ND). Both periglomerular cells and short-axon cells were observed with both techniques employed, and their colocalization in the same neurons demonstrated that ND is a reliable marker for NOS-expressing cells in the mouse olfactory bulb (OB). The histochemical technique differentiates two types of glomeruli: ND-positive and ND-negative. Olfactory glomeruli in the CD-1 strain were about 7% larger than those in the BALB/c animals. While the density of NOS/ND-containing periglomerular cells was similar between both strains studied, more NOS/ND-labelled cells were observed in the ND-positive glomeruli ($P = 0.002$). Since periglomerular cells in the BALB/c strain do not receive direct olfactory receptors synapses, the present results indicate that such inputs do not regulate the expression of NOS and ND activity in the periglomerular cells. The different densities of NOS/ND-expressing periglomerular cells may indicate that nitric oxide is implicated in a differential modulation of the odor response within both types of chemically distinct glomeruli in the mouse olfactory bulb. J. Neurosci. Res. 53:239–250, 1998.

Key words: BALB; CD-1; olfactory bulb; immunohistochemistry

INTRODUCTION

The olfactory bulb (OB) is the first relay station in the processing of olfactory information. Axons from receptor cells in the olfactory mucosa make synaptic contacts within the olfactory glomeruli mainly on dendrites from mitral cells and tufted cells, but also onto different types of interneurons, including periglomerular cells, external tufted cells, and diverse superficial and deep short-axon cells (Macrides and Davis, 1983; Halász, 1990).

Two mouse strains, BALB/c and CD-1, differ in the connectivity of their OBs. Olfactory receptor cells establish synaptic contact onto periglomerular cells in the CD-1 strain but not in the BALB/c mice (White, 1972, 1973). There are also quantitative variations, including higher number of catecholaminergic neurons in the OB of the BALB/c mouse as compared to CD-1 animals (Baker et al., 1980, 1983a). Additional differences between both strains are reflected in their distinct response to chemical olfactory deafferentation. Following receptor cells lesions, the levels of tyrosine hydroxylase in the OB are reduced in both strains, but this reduction is considerably more severe in CD-1 mice than in BALB/c animals, whether analyzed immunohistochemically or biochemically (Baker, 1988).

Nitric oxide synthase (NOS) is the key enzyme to produce nitric oxide, a novel diffusible messenger involved in neurotransmission and neuromodulation in normal and pathological brain (for reviews see Förstermann and Kleinert, 1995; Jaffrey and Snyder, 1995; Wolf, 1997). Nicotinamide adenine dinucleotide phosphate (NADPH)-diaphorase (ND) is a selective marker for distinct neural populations widely distributed in the central nervous system (Vincent and Kimura, 1992).

Contract grant sponsor: Junta de Castilla y León; Contract grant sponsor: DGICyT; Contract grant number: PB94–1388.

*Correspondence to: Dr. José R. Alonso, Dpto. Biología Celular y Patología, Universidad de Salamanca, E-37007 Salamanca, Spain. E-mail: jralonso@gugu.usal.es

Received 6 August 1997; Revised 3 March 1998; Accepted 10 March 1998

Using NADPH as cosubstrate and tetrazolium salts as chromogen, ND activity can be localized in fixed and unfixed brain tissue (Thomas and Pearse, 1961; Alonso et al., 1995a). ND activity and neuronal NOS (NOS I; EC 1.14.13.39) immunoreactivity widely colocalize in astrocytes and specific sets of well characterized neurons in the central nervous system (Bredt et al, 1991a; Hope et al., 1991; Kishimoto et al., 1993; Kugler and Drenckhahn, 1996). The staining of glial cells can be eliminated by a strong fixation with paraformaldehyde (Gabbott and Bacon, 1996); hence, in most cases, ND histochemistry is an easy method to display neurons producing the neuroactive molecule nitric oxide.

The distribution of ND activity in the OB has been established in different mammals: rat (Davis, 1991; Vincent and Kimura, 1992; Alonso et al., 1993), hamster (Davis, 1991), mouse (Kishimoto et al., 1993), hedgehog (Alonso et al., 1995b), and primates (Alonso et al., 1996). A common ND-staining pattern has been observed in the OB of these species: olfactory fibers and glomeruli, different types of intrinsic interneurons, and centrifugal fibers. While in rodents and insectivores, ND-positive glomeruli have a clear-cut distribution only in the rostral and dorsomedial portions of the OB, all olfactory fibers and glomeruli are ND-positive in the primate OB (Alonso et al., 1996). However, this ND staining in olfactory fibers and glomeruli is NOS-immunonegative in adult rodents (Kishimoto et al., 1993; Kulkarni et al., 1994; Roskams et al., 1994). That histochemical activity may correspond to other enzymes with close homology with NOS such as cytochrome P-450 reductases (Bredt et al., 1991b; Knowles and Moncada, 1994), or to an immunologically distinct form of NOS (DellaCorte et al., 1995). On the other hand, all the ND-labelled interneurons in the OB colocalize NOS and NOS mRNA (Kishimoto et al., 1993).

Whereas variations in the ND staining pattern between different groups of mammals or between different species of rodents are known, there are no available data about possible differences between more closely related systems, such as OBs of well-studied strains of the same species. Therefore, the aim of this work is to compare qualitatively and quantitatively the ND and NOS staining patterns in the mouse olfactory bulb between the BALB/c and CD-1 mouse strains, and between the two chemically distinct sets of glomeruli, ND-positive and ND-negative.

MATERIALS AND METHODS

Adult female mice (*Mus musculus*) were used for this study. Five animals of each strain (CD-1 and BALB/cByJIco; Criffa S.A., Barcelona, Spain) were deeply anesthetized (Ketolar, 50 mg · kg^{-1} b.w.) and perfused through the ascending aorta. The blood was washed out with saline for 30 sec followed by a fixative containing 4% (w/v) depolymerized paraformaldehyde and 15% (v/v) saturated picric acid in 0.1 M phosphate buffer, pH 7.4 (PB) for 20 min. The OBs were immersed for 2 hr at 4°C in the perfusate and rinsed thoroughly with PB. The tissue was cryoprotected with 30% (w/v) sucrose in PB, quickly frozen in melting isopentane and cut in a cryostat at 30 µm at the coronal plane. Serial sections were processed for: (a) ND histochemistry, (b) NOS immunohistochemistry, or (c) NOS/ND double-labelling. The stained sections were mounted on gelatin-coated slides and coverslipped with phosphate-buffered glycerol or were dehydrated and coverslipped with Entellan™.

NADPH Histochemistry

ND technique was performed as described previously (Kishimoto et al., 1993; Alonso et al., 1995b), slightly modified. Free-floating sections were incubated in two steps. First, in a medium containing 0.3% (v/v) Triton X-100, 0.1 mM nitroblue tetrazolium (NBT; Sigma, St. Louis, MO) and 1.2 mM β-NADPH (tetrasodium salt, Sigma) in phosphate-buffered saline (PBS), pH 8.0 during 60–90 min at 37°C. After rinsing in cold PB, the tissue was again incubated in a medium containing 0.08% Triton X-100, 1 mM nitroblue tetrazolium, and 1.2 mM β-NADPH in Tris-HCl buffer, pH 8.0, for 30–40 min, at 37°C. The reactions were controlled under the microscope and stopped with cold PB. Controls for specificity of the ND histochemistry were carried out as previously described (Alonso et al., 1992, 1995a). No reaction product was observed in the tissue when incubated without NADPH or without chromogen.

Nitric Oxide Synthase Immunohistochemistry

Free-floating sections were incubated at 4°C for 3 days in the primary antiserum (anti-NOS I, 1:20,000) with 10% normal rabbit serum and 0.05% Triton X-100 in PBS, pH 7.4. Biotinylated anti-sheep IgG (Vector, Burlingame, CA, 1:200 in PBS) was applied for 60 min and the Vectastain ABC complex (Vector, 1:250 in PBS) for 90 min, both at room temperature. Tissue bound peroxidase was revealed incubating the tissue with 0.003% H_2O_2 and 0.05% 3,3'-diaminobenzidine (DAB) in 0.05 M Tris-HCl buffer, pH 7.6, the reaction being controlled under the microscope. After each incubation, the sections were thoroughly rinsed in PBS (4 × 10 min), at room temperature.

The polyclonal K205 antiserum was raised against purified rat recombinant NOS I expressed in a baculovirus/insect cell system (for specificity details see Herbison et al., 1996). Antisera specificity controls were performed in

some of the series by omitting the primary antisera. No residual reaction was observed.

NADPH Histochemistry/Nitric Oxide Synthase Immunohistochemistry Double-Staining

Sections were first processed for NOS immunohistochemistry. The first antiserum was detected with fluorescein isothyiocyanate (FITC)-conjugated anti-sheep serum (Vector, 1:50 in PBS; 2 hr), and photographs of select fields were taken. Immediately after, the selected sections were thoroughly rinsed in PB and processed for ND histochemistry as described above. The same fields as for NOS immunofluorescence were photographed with bright-field microscopy.

Quantitative Analysis

From each ND-stained series, 24 sections were randomly selected. For each section, the mitral cell layer was outlined with a camera lucida using a 6.3× objective. The resultant areas comprising the inframitral layers (including inner plexiform layer, granule cell layer, and white matter of the main olfactory bulb, and excluding the area corresponding to both the accessory olfactory bulb and the anterior olfactory nucleus) were calculated with a MOP-Videoplan image analysis system (Kontron, Munich, Germany). The number of labelled deep short-axon cells was counted in each section, and their densities respecting their inframitral layers were calculated. Major diameters of the different labelled neuronal types were calculated using the same equipment.

Each coronal section was divided in eight quadrants as follows: dorsal, dorsolateral, lateral, ventrolateral, ventral, ventromedial, medial, and dorsomedial. Two or six glomeruli (see below) were randomly chosen in each section and their topographical locations within the bulb were noted. Seemingly to the inframitral areas, the glomerular limits were outlined and their perimeters were measured. Randomly chosen glomeruli with doubtful limits were discarded and their immediately neighboring ones employed for quantification. ND-labelled periglomerular cells around glomeruli with well-defined third-order dendrites were counted, and the densities respecting their glomeruli were calculated. Those periglomerular cells (PG) with dendrites entering two glomeruli were not included in the quantification. Only the rostralmost sections displayed ND-positive and ND-negative glomeruli. Hence, we analyzed four ND-positive glomeruli and two ND-negative glomeruli in each of the 12 rostralmost sections, but only two ND-negative glomeruli in the 12 caudalmost sections of each series. The same number of both ND-type of glomeruli, sections, and animals were analyzed for both mouse strains: 48 ND-positive and 48 ND-negative glomeruli in each OB, with a total of 240 glomeruli of each ND-type and each mouse strain. Three parameters were statistically studied: (1) density of labelled deep-short-axons cells in inframitral layers; (2) glomerular size; (3) density of labelled periglomerular cells.

We used nonparametric tests to determine whether or not groups constituted homogeneous populations. The Kruskal-Wallis test was employed to compare each parameter (a) between rostrocaudal levels, and (b) between topographical locations. Mann-Whitney-U-tests were employed to compare the parameters (a) between strains and (b) between ND-positive and ND-negative glomeruli. Values are expressed as mean ± S.E.M. In all tests, *P*- values less than 0.05 were considered significant for differences.

RESULTS

The staining patterns of ND histochemistry and NOS immunohistochemistry in the olfactory bulb of both mouse strains, CD-1 and BALB/c, were essentially similar. Firstly, we describe the qualitative common morphological characteristics, and thereafter the quantitative results.

NOS immunohistochemistry and ND histochemistry provided a staining of cells and fibers enabling a clear morphological characterization of positive elements. ND histochemistry and NOS immunohistochemistry colocalized in the same cells throughout the mouse OB, as demonstrated with the double-labelling method (Fig. 1). However, labelled fibers and dendrites appeared generally less defined with NOS immunohistochemistry as compared with the histochemically labelled elements, which presented a Golgi-like definition. The sections processed with immunohistochemistry displayed higher nonspecific background and the labelled elements were stained more uniformly. By contrast, a wide range of degrees of staining between the different labelled types were seen after ND histochemistry. Both types of staining were present in numerous interneuronal types located in the glomerular layer (GL) and in a few scattered neurons located in the external plexiform layer (EPL), inner plexiform layer (IPL), and granule cell layer (GCL).

Neuropil staining was evident in all layers, but particularly dense in specially located glomeruli and the corresponding olfactory nerve bundles after ND staining (Figs. 2 and 3). All olfactory fibers and their arborizations in the glomeruli were NOS-immunonegative. After the first ND incubation step described in the present work, only cell somata and neurites appeared well defined, and ND-positive glomeruli displayed strong histochemistry reaction only when the second incubation step was accomplished. The histochemical reaction was sensitive to the time between sectioning and the incubation, and the

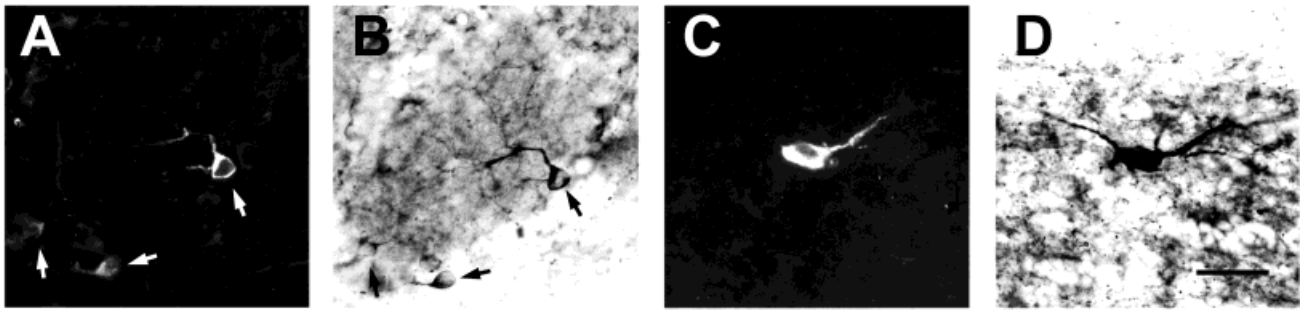

Fig. 1. Nitric oxide synthase (NOS) immunohistochemistry-NADPH-diaphorase (ND) histochemistry double labelling in the mouse olfactory bulb. **A** and **C** show NOS-immunoreactive elements after fluorescein isothiocyanate (FITC)-labelled indirect immunofluorescence. **B** and **D** are micrographs from the same fields shown in A and C, respectively, with brightfield microscopy after ND staining. Arrows in A and B point to periglomerular cell (PG) somata displaying both NOS immunohistochemistry and ND staining. C and D fields are centered in the granule cell layer (GCL), showing a deep short-axon cell after the double staining. Note a better definition of positive fibers after ND staining. Scale bar = 25 μm.

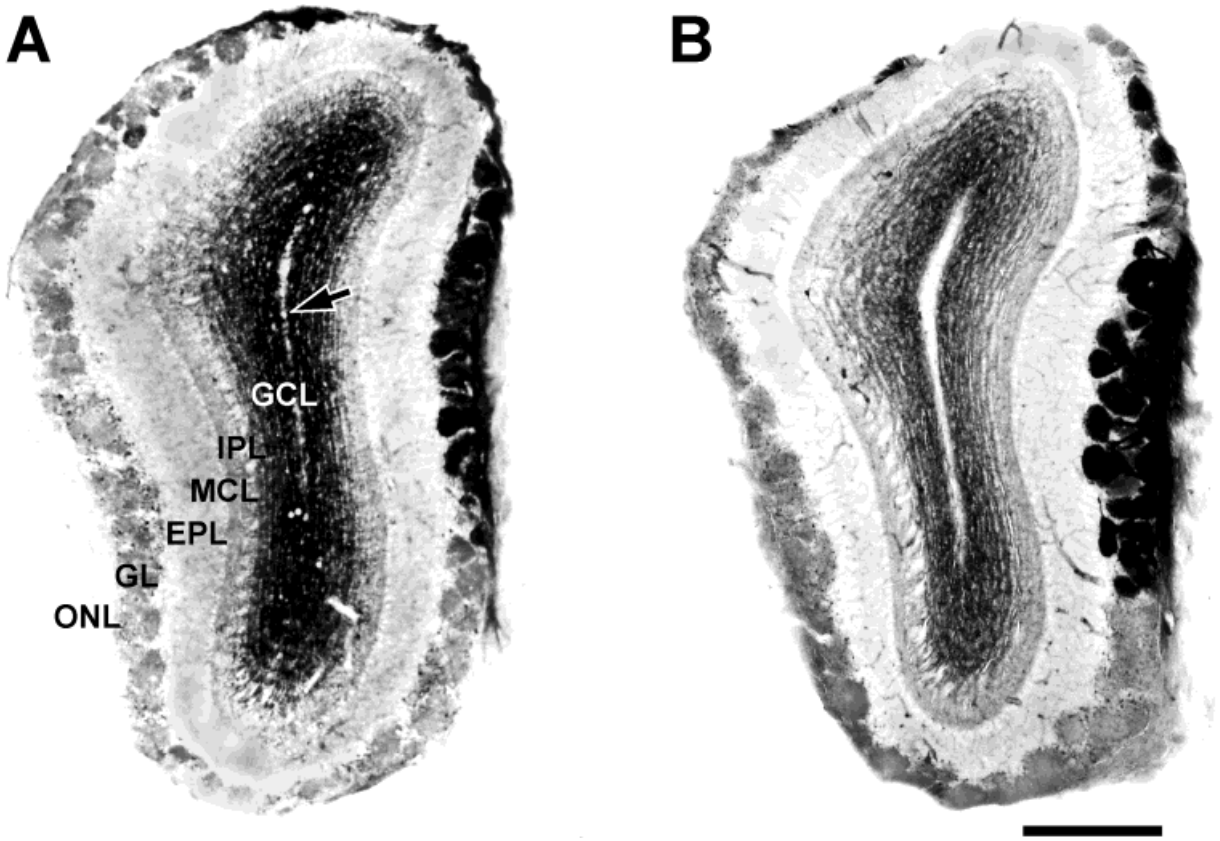

Fig. 2. Panoramic views of coronal sections of the mouse olfactory bulb stained for ND activity. **A** is from CD-1 strain and **B** from BALB/c. Note the profuse fiber staining in the inframitral layers (inner plexiform layer [IPL] + granule cell layer [GCL]) but not in the white matter (arrow). At this rostrocaudal level, ND-positive glomeruli are medial and dorsomedially located. Up is dorsal, right is medial. ONL, olfactory nerve layer; GL, glomerular layer; EPL, external plexiform layer; MCL, mitral cell layer. Scale bar = 0.5 mm.

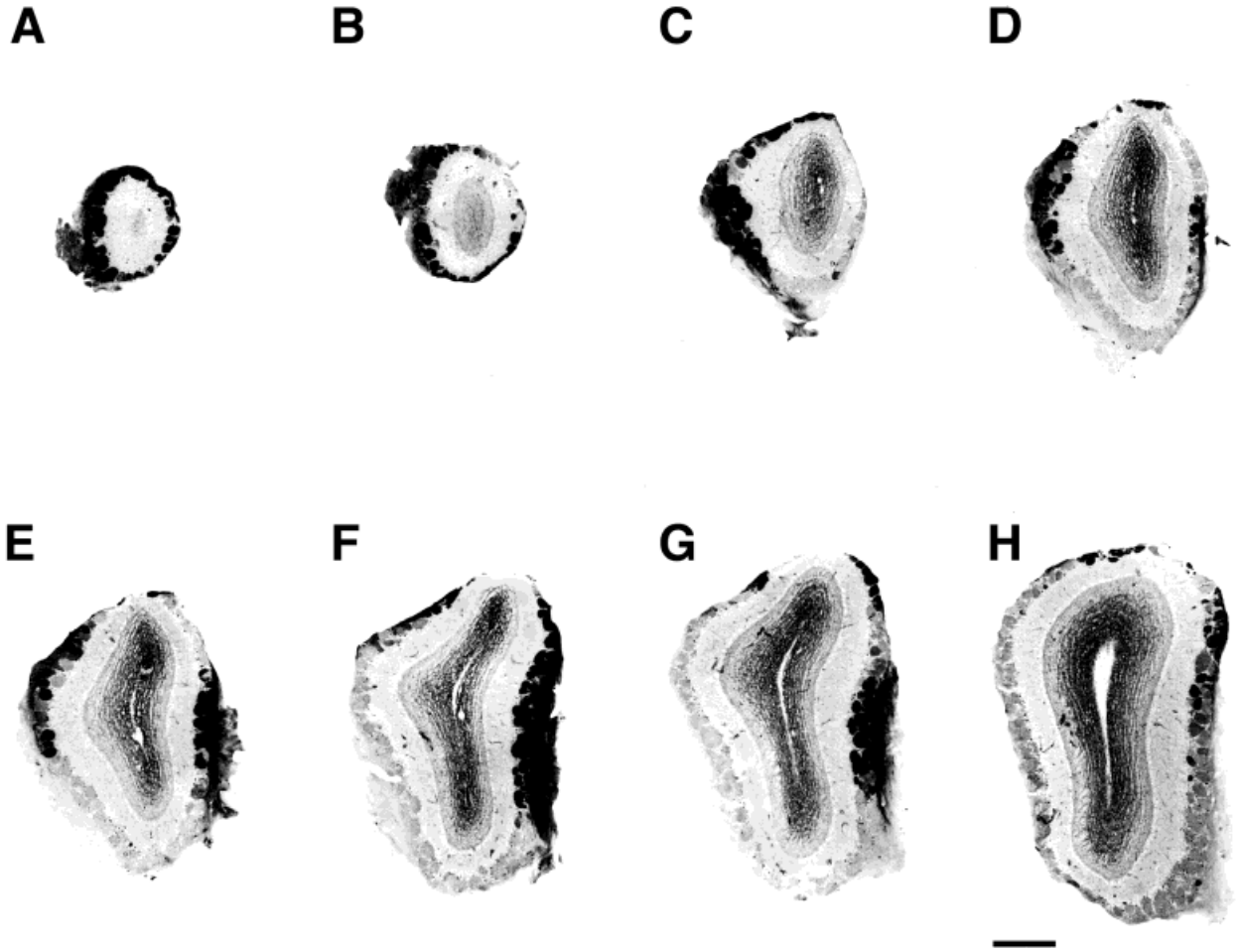

Fig. 3. Spatial distribution of the ND-positive glomeruli among the mouse olfactory bulb (OB; BALB/c strain) as seen in 30-µm-thick coronal sections. ND-positive glomeruli are localized in the rostral half of the OB. In the rostralmost level (**A**) all glomeruli are positive. More caudally, these glomeruli are set as a continuous rim from the dorsal to the ventromedial parts (**B**) and between the dorsal to ventral parts (**C**). From this point to the caudal region, the ventral and ventrolateral locations are free of ND-positive glomeruli, these ones being located by the lateral, dorsolateral, dorsomedial, and medial parts (**D**-**H**). At these levels, some ND-negative glomeruli are grouped at dorsal locations or intermingled with the ND-positive ones. Most ND-positive glomeruli are located at the medial border of the OB (E-G; see Fig. 2). At midrostrocaudal levels of the OB, only a few dorsomedial ND-positive glomeruli can be seen (H). In each photograph, up is dorsal and right is medial. Scale bar = 0.5 mm.

quality of the reaction drastically decreased after a week, or when sections were employed for other techniques (i.e., double-staining NOS-ND). The second incubation step alone (i.e., high concentration of NBT) yields a good staining of ND-positive glomeruli, but we obtained better definition of the positive cells using the first incubation step (i.e., low concentration of NBT) in the mouse OB. Hence, we used the combination of NOS immunofluorescence and only the first incubation step of ND histochemistry to demonstrate colocalization in the neurons (Fig. 1).

The ND-positive glomeruli had a special location in the mouse OB deduced from the serial coronal sections. Briefly, they were found only in the rostralmost half of the OB and they are set in different locations at the different rostrocaudal levels (Fig. 3).

In the glomerular region, three types of NOS/ND-stained cells were distinguished. First, stained PG (Fig. 4) were numerous, with small somata (9.3 $\pm$ 0.1 µm). Only a thin rim of cytoplasm was visible, and the dendrites branched within a single glomerulus and rarely in two. Only those PG with well-visible third-order dendrites were used for quantification, the pertaining glomeruli being easily ascribed (Fig. 4A,B). The few PG branching into two glomeruli were not included in the quantification. A second type of NOS/ND neurons appeared in the inner part of the GL and in the superficial EPL. They

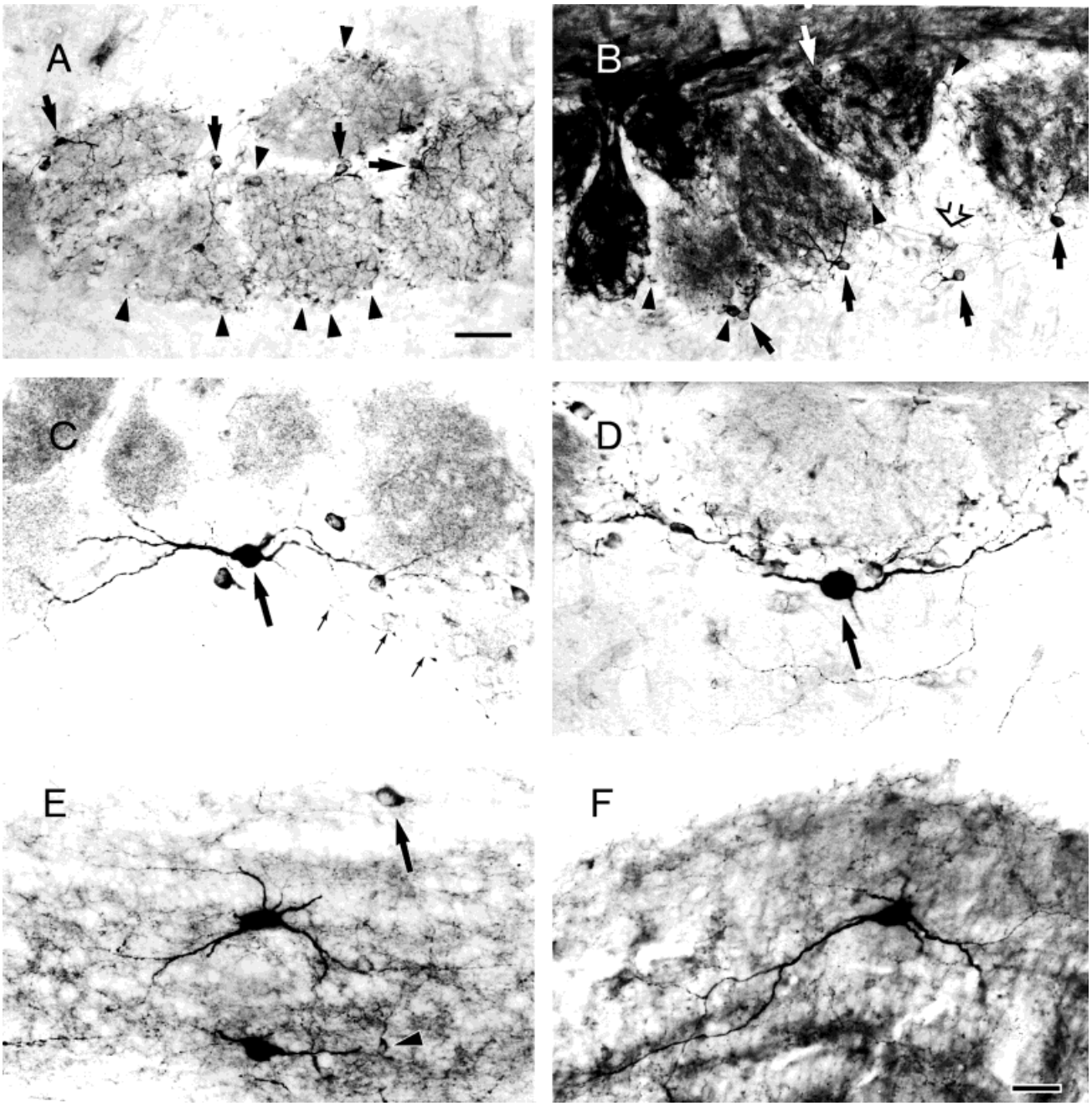

Fig. 4. ND-positive elements in the mouse olfactory bulb. Left panels correspond to CD-1 strain while the right ones to BALB/c animals, but all represented elements are present in both strains. A-D are fields centered in the glomerular region. In **B**, ND-positive glomeruli are seen, whereas only ND-negative glomeruli are shown in **A, C,** and **D**. The limits of these anatomical structures are easily distinguished, even in the ND-negative ones. Note that ND-labelled PG are located around both types of glomeruli (arrows and arrowheads), but only those PG with well-defined third-order dendrites (arrows) were included in the statistical analysis. Faintly stained PG (arrowheads) were difficult to quantify: their dendrites were frequently not stained and thus the assignation of PG to a specific glomerulus was unreliable. In C and D, large arrows indicate positive superficial short-axon cells. Note the axon of the cell in C running through the external plexiform layer (EPL; small arrows). **E** and **F** show ND-labelled deep short-axon cells in the granule cell layer (GCL). Arrow in E points to a weakly stained cell (included in the quantitative analysis). A granule cell can be seen (arrowhead) intermingled with the ND-positive neuropil. Scale bars = 50 μm (A and B); 25 μm (C–F).

showed a dense formazan reaction product (Fig. 4C,D). The oval or fusiform somata had larger size (17.2 ± 0.8 μm) than the PG and several dendrites ramifying mainly in the GL and superficial EPL, without entering within the glomeruli. These cells, identified as superficial short-axon cells, were not included in the statistical analysis because of their low number (8–12 per whole olfactory bulb). The third type of NOS/ND-positive neurons in this region was very scarce, and long incubations were necessary to stain them, with either ND histochemistry or peroxidase staining for NOS immunolabelling. No stained dendritic trees could be observed, and therefore they could not be classified with certainty (Fig. 4B). According to their size and location, they may correspond to superficial short-axon cells or external tufted cells. Neuropil in the outer layers of the bulb (aside from the olfactory axons) was constituted by a few solitary NOS/ND-positive fibers coursing without predominant orientation.

In the inframitral layers, two main types of NOS/ND neurons were observed. The first one appeared scattered in the GCL, rarely in the IPL, and in the inner part of the EPL. Their somata (major diameter 7.8 ± 0.1 μm) showed a narrow cytoplasmic rim and a thin, long dendrite that coursed perpendicular to the OB layering. They were identified as granule cells. These neurons were faintly stained and intermingled with the dense NOS/ND-labelled neuropil present in this region, making unreliable their proper quantification (Fig. 4E). Moreover, for granule cells, a total colocalization of NOS and ND was uncertain because of the reasons pointed above. Otherwise, the rest of neurons in the mouse OB displaying ND-activity clearly colocalize NOS immunoreactivity. The second neuronal type was larger (18.2 ± 0.5 μm) and these cells were located in the GCL, and less frequently in the mitral cell layer (MCL), IPL and white matter (WM). All these large cells in the inframitral layers were typified as deep short-axon cells (Fig. 1C,D). These neurons had oval, fusiform, or polygonal cell bodies, with several thick, long, barely branched dendrites that coursed without defined orientation. ND histochemistry revealed different degrees of staining for different subtypes of deep short-axon cells (Fig. 4E,F) while with NOS immunohistochemistry, all their somata displayed about the same staining intensity. In the inner regions of the OB, a laminar pattern of NOS/ND staining was observed in the inframitral layers, being more defined with ND technique. In these layers, a decreasing NOS/ND staining gradient was observed from the border of the WM with the GCL to the MCL. Only a few NOS/ND-reactive fibers were found in the WM (Fig. 2).

Quantitative Analysis

In the CD-1 strain, the density of deep short-axon cells in 30-μm-thick sections was 6.577 ± 0.356 cells · mm^{-2} and in the BALB/c mice 5.682 ± 0.297 cells · mm^{-2}. A Mann-Whitney-U-test did not detect a statistical significant difference between both groups ($P = 0.079$). When histograms of the density of deep short-axon cells at different rostrocaudal levels were built, they showed a more or less homogeneous distribution of that parameter along the length of the OB, with a slight increase at the central region of the OB (not shown). However, the Kruskal-Wallis test did not detect statistical significant differences among the different rostrocaudal levels ($P = 0.056$).

The second parameter subjected to statistical analyses was the glomerular perimeter as indicator of their size. In CD-1 mice, the glomerular perimeter was 274.8 ± 2.6 μm, and 256.1 ± 2.2 μm in BALB/c olfactory bulbs (Table I). After performing the Mann-Whitney-U-test, no difference was detected between the size of ND-positive and ND-negative glomeruli ($P = 0.346$). However, the same test betrayed a highly significant difference between the glomerular size of both strains ($P < 0.0001$), the CD-1 glomeruli being larger than those of BALB/c mice. With the Kruskal-Wallis test we also detected differences in the glomerular perimeter between the different topographical locations ($P = 0.028$ for CD-1 and $P < 0.0001$ for BALB). This parameter also showed differences between the different rostrocaudal levels in the CD-1 mice ($P = 0.005$) but, surprisingly, the glomerular size was homogeneous along the rostrocaudal axis in the BALB strain ($P = 0.651$).

Concerning the density of ND-labelled PG, the Mann-Whitney-U-test did not detect statistical differences between data sets of PG densities from both strains ($P = 0.133$), but it did between data from ND-positive and ND-negative glomeruli ($P = 0.002$; Table II). Further analyses also showed the same results when the Mann-Whitney-U-test was applied separately within each strain or within each ND-type of glomeruli (not shown). The density of NOS/ND periglomerular cells around glomeruli presented differences between rostrocaudal levels ($P = 0.003$) and between topographical locations ($P = 0.0001$; P values for Kruskal-Wallis tests).

TABLE I. Glomerular Size*

	CD-1	BALB/c	Both strains
ND+[a]	277.8 ± 3.6	256.9 ± 3.3	267.4 ± 2.5
ND−	271.7 ± 3.8	255.2 ± 2.9	263.5 ± 2.4
ND+ and ND−	274.8 ± 2.6	256.1 ± 2.2	

*Comparison of Glomerular Size (glomerular perimeter [μm] from 30-μm-thick coronal sections) of ND-positive (ND+) and ND-negative (ND−) glomeruli, in both mouse strains, CD-1 and BALB/c. Values are presented as mean ± S.E.M. for each group. Mann-Whitney tests detected significant differences between glomeruli from both strains ($P < 0.0001$) but not between ND-positive and ND-negative glomeruli ($P = 0.346$).

[a]ND, NADPH-diaphorase.

TABLE II. Densities of ND-Labelled Periglomerular Cells*

	CD-1	BALB/c	Both strains
ND+[a]	4.141 ± 0.241	4.435 ± 0.244	4.288 ± 0.171
ND−	3.272 ± 0.181	3.726 ± 0.209	3.499 ± 0.139
ND+ and ND−	3.706 ± 0.152	4.080 ± 0.161	

*Comparison of lineal densities of nitric oxide synthase (NOS)/ND-labelled PG (number of cells per mm of glomerular perimeter, in 30-µm-thick coronal sections) around ND-positive (ND+) and ND-negative (ND−) glomeruli, in both mouse strains, CD-1 and BALB/c. Values are presented as mean ± S.E.M. for each group. Mann-Whitney tests detected significant differences between ND-type glomeruli ($P = 0.002$) but not between strains ($P = 0.133$). The same tests between subgroups confirmed these results (data not shown).
[a]ND, NADPH-diaphorase.

In conclusion, statistical analysis demonstrated that there are more NOS/ND-labelled PG around ND-positive glomeruli (4.288 ± 0.171 cells · mm^{-1}) than around ND-negative ones (3.499 ± 0.139 cells · mm^{-1}) in the mouse OB (Table II).

DISCUSSION

Both mouse strains studied, CD-1 and BALB/c, present differences in the organization of their periglomerular region, but they showed similar NOS/ND-containing neurons in the main OB, as revealed by NOS immunohistochemistry and by NADPH-diaphorase histochemistry. The density of ND-labelled PG around ND-positive and ND-negative glomeruli was different in both strains.

Differences in the size of the glomeruli were found between both strains, independent of their chemical phenotype (ND-positive or ND-negative). It is interesting to note that the glomerular and general OB sizes diminished when animals underwent experimental deafferentation by both surgical disruption of the peripheral olfactory inputs or chemical destruction of the olfactory epithelium (Nadi et al., 1981; Baker et al., 1983b, 1984; Meisami and Hamedi, 1986; Ehrlich et al., 1990). In our observations, the BALB/c strain, which lacks synaptic contacts from olfactory receptor cells axons onto PG, has smaller glomeruli than those in the CD-1 strain, where synaptic contacts between olfactory axons and PG are present (White, 1972, 1973). Moreover, differences in the glomerular size have been shown in the mouse OB along the rostrocaudal axis, those located in midrostrocaudal levels being larger (Royet et al., 1988). We also found such differences, but only in one of the strains studied. A possible explanation for all these divergences in the glomerular size would be that the glomeruli of different levels (Royet et al., 1988), or from both strains develop at different rates. It has been described an at least 5-day delay of onsets of both brain growth and standard learning test in the BALB/c mice compared to the CD-1 strain (Epstein et al., 1991). However, both parameters reach the adult values at 23 days old. Our animals were older (3 months) and, thus, the differences in glomerular size do not reflect ontogenetic phenotypic variations but real intraspecies differences.

The distribution of ND-positive elements in the OB is extensively documented in the rat and hamster (Davis, 1991; Vincent and Kimura, 1992; Alonso et al., 1993). Only the work of Kishimoto et al. (1993) provides specific information about the distribution of NOS/ND in the mouse OB. The general distribution pattern of NOS/ND elements in the OB is in accordance with this study, but the coincidence in the same cells of both the enzyme and the ND activity is here directly proved by the double-labelling method. Also, variations in the rostrocaudal and topographical location of the ND types of glomeruli are here described for the first time. We also modified the ND technique by combining methods described elsewhere (Kishimoto et al., 1993; Alonso et al., 1995a). Hence, the use of the related specific fixation conditions and the first incubation step alone (with low concentrations of NBT and PBS) allows the labelling of only NOS-immunoreactive neurons with the histochemical technique, as proved by the double-staining method. Type of fixation is determinant for the ND-staining pattern but not for NOS immunoreactivity in brain (Buwalda et al., 1995). Moreover, astrocytes are ND-positive and immunoreactive for NOS I when the tissue is submitted to a weak fixation with aldehydes, but the labelling is restricted to neuronal elements when that step is enhanced (Gabbott and Bacon, 1996; Kugler and Drenckhahn, 1996). Kishimoto et al. (1993) stained ND-positive glomeruli in the mouse OB using the same incubation medium described in this work; such divergence could arise from differences in the fixation and incubation times.

Croul-Outman and Brunjes (1988) indicate that the rostrocaudal distribution of ND-stained short-axon cells in the rat OB is relatively uniform, whereas an increase in the rostral border between the accessory and main OBs has been, by contrast, reported (Scherer-Singler et al., 1983; Scott et al., 1987). This border is located approximately in the midrostrocaudal level of the OB, where we also quantitatively reported such variability. However, the statistical analysis showed a uniform density of NOS/ND-labelled deep short-axon cells among the entire mouse OB. No differences in the connectivity between both strains have been described in zones deeper than the glomerular layer. Moreover, such peculiarities in the olfactory glomeruli are unlikely to affect directly the deep short-axon cells, since the main inputs to the latter interneurons come from centrifugal fibers (see Halász, 1990). In the present report we demonstrate differences in

the density of NOS/ND-marked PG interneurons along the rostrocaudal axis. These differences are probably related to the variations existing between ND-positive and ND-negative glomeruli, the latter located mostly in the rostralmost part of the OB (see below). Our results, indicating that there are no differences between the distribution of deep short-axon cells in CD-1 and BALB/c animals, may suggest that these second-order interneurons are not severely affected by the differences in the glomerular circuitry in both mouse strains.

Tract-tracing methods, immunohistochemical markers, and lectin-binding markers bring up the hypothesis of a functional organization of the projections from the receptor cells to the OB (Breer and Shepherd, 1993; Shepherd, 1994; Crespo et al., 1996; Porteros et al., 1996). Spatial specific projections from subclasses of chemically heterogeneous olfactory receptor cells are studied in rodents (Mori, 1987; Key and Akeson, 1991; Schwarting and Crandall, 1991; Schwarting et al., 1992). Specific cell surface glycoconjugates (CC2 antigens) are expressed in the OB only in dorsomedially located glomeruli until adulthood, as well as in the olfactory nerve layer at the rostral part of the OB (Schwarting et al., 1992). DellaCorte et al. (1995) found ND activity in olfactory receptor neurons in specific regions within the olfactory epithelium of the rat. The corresponding glomerular ND staining here reported in the mouse overlaps partially with the distribution pattern of CC2.

Our results indicate that there are more NOS/ND-positive PG around ND-positive glomeruli than around the negative ones. This finding supports the hypothesis that both kinds of glomeruli are chemical and functionally different. Studying the distribution of ND-positive elements in the hamster and rat, Davis (1991) indicates that in the former, the PG somal staining was uniform through all the glomeruli. Thus, a difference regarding the number of ND-positive PG between the ND-positive glomeruli (dorsal; see above) and the ND-negative ones (ventral) is not evident. On the other hand, Davis (1991) found in the rat OB less ND-stained PG in the ventral part (where glomeruli are predominantly ND-negative) than in the dorsal part (predominantly ND-positive). Even though such analyses were only qualitative, these findings indicate interspecies differences within rodents. In the mouse OB, the Kruskal-Wallis analysis demonstrates differences of the density of NOS/ND-PG both between topographical locations and between rostrocaudal levels. ND-positive glomeruli in this species are localized, as we pointed out before, in the rostralmost half of the bulb and in different locations depending on the rostrocaudal level (see Fig. 3). Thus, the differences in the density of NOS/ND-labelled PG at different topographical locations may be easily explained because of the peculiar distribution of the chemically identified glomeruli. Quantitative studies from our group on the distribution of ND-active PG in the rat show opposite results to those of Davis (1991), as no differences were found between ND-positive and ND-negative glomeruli (Alonso et al., 1993; Crespo et al., 1996). By contrast, a topographical variability of glomeruli in the mouse is quantitatively demonstrated in the present work.

Olfactory glomeruli may be subdivided into typical and atypical glomeruli, the latter defined by differences in their ultrastructure, the spatial distribution of primary olfactory axons within the glomeruli, and by an intense and early cholinergic innervation from centrifugal fibers (Zheng and Jourdan, 1988; Le Jeune and Jourdan, 1991, 1993). Clear differences in the distribution of NOS/ND-active PG around typical (both ND-positive and negative) and atypical (only ND-negative) glomeruli were also found (Crespo et al., 1996). Because of their scarce number in the OB, the atypical glomeruli in the OB may very unlikely have a statistical influence on our results.

NOS exists in a subpopulation of PG in the mouse OB (Kishimoto et al., 1993; Roskams et al., 1994; present study). Breer and Shepherd (1993) proposed that nitric oxide, by the induction of cGMP signals, could modulate the neural response to odour stimulation at the glomerular level. They proposed that single glomeruli, including their PG, could function as ''closed'' and independent units where nitric oxide could diffuse and act. The spatial segregation of NOS/ND-positive PG found in this report implicates that NO may be present in a higher concentration in the ND-positive glomeruli of the mouse OB. Such differences could be explained as directly or indirectly involving nitric oxide in the activity of these particular glomerular subsets. Roskams et al. (1994) provide evidence in vivo that NOS may function in activity-dependent pattern formation and maintenance of neuronal projections in the developing and regenerating olfactory system. However, DellaCorte et al. (1995) suggest the presence of an immunologically different form of NOS in rat olfactory epithelium and glomeruli also in adulthood. As NO acts as a diffusible retrograde messenger (Bredt and Snyder, 1992; Breer and Shepherd, 1993; Dawson, 1995; Wolf, 1997), a different regulation towards the peripheral olfactory axons in both types of glomeruli may be possible.

Recent studies indicate that the distribution of NOS is not static, but rather dynamically regulated by neuronal activity (Matsumoto et al., 1993), nerve growth factors (Hirsch et al., 1993), and neuronal damage and regeneration (Verge et al., 1992; Wu, 1993; Solodkin et al., 1992; Vizzard et al., 1993; Roskams et al., 1994). Besides, the olfactory epithelium has enormous inductive capacity and trophic action in the mammalian brain, as the respective olfactory axons are able to produce ectopic glomeruli even in the frontal cortex (see Dryer and

Graziadei, 1994). Thus, the different densities of NOS-containing PG around ND-types of glomeruli could reflect the differences in the chemical content of the ND-positive and ND-negative axons and the respective olfactory receptor cells (for review see Lewin, 1994).

Peripheral afferences did not establish axodendritic synaptic contacts with PG in BALB/c mice, and the number of NOS-containing PG were found not to be different between both strains studied. The phenotypic expression of NOS/ND in these cells seems to be independent from the direct excitatory inputs from the olfactory receptors neurons. Perhaps the expression of NOS is controlled by indirect olfactory inputs (via the mitral cells) or by trophic factors and modulators present in different concentrations within both types of glomeruli.

The two mouse strains studied also displayed other neurochemical differences. The BALB/c mice has higher tyrosine hydroxylase (TH) activity and/or dopamine levels in all brain regions (Baker et al., 1980, 1983b) compared with the CD-1 strain. Such differences are directly reflected in a higher number of TH-stained juxtaglomerular neurons in the BALB/c OB, as it has been demonstrated using immunohistochemistry. When both strains undergo chemical olfactory receptor lesions, BALB/c mice continue expressing TH, even though the levels are slightly reduced. However, CD-1 mice showed a drastic reduction in the number of TH-labelled juxtaglomerular neurons after the lesion (Baker, 1988). This reduction in TH immunoreactivity did not appear to be associated with cell death. TH-positive neurons also express DOPA-decarboxylase in normal conditions, and, after olfactory deafferentation, these neurons still express the latter enzyme without depletion, and dopamine synthesis was still observed following exogenous administration of L-DOPA (Baker et al., 1983b, 1984). Inhibition of odorant-induced afferent activity by naris closure also profoundly reduces TH expression in juxtaglomerular neurons of CD-1 mice (Baker et al., 1993). These results support the hypothesis that odor sensory activity, peripheral olfactory innervation, and intrabulbar connections are required for the expression of the TH phenotype in the OB. Notwithstanding these observations, naris closure does not affect ND activity in short-axon cells in the rat OB (Croul-Ottman and Brunjes, 1988). In the rat OB, ND activity, TH- and calbindin D-28k immunoreactivity are expressed in PG. ND activity does not colocalize either with TH (Johnson and Ma, 1993), or with calbindin D-28k (Alonso et al., 1993). These findings are qualitatively similar in the mouse OB (unpublished data). Thus, different subpopulations of PG can be distinguished in relation to their chemical content. While a reduction in the TH-containing PG after lesion is clear, the effects of similar experiments on the NOS/ND-active subpopulation could help to understand the regulation of its expression. In this sense, the experiments on Purkinje cell death (PCD) mice, which lack afferences from mitral cells onto PG by a specific loss of the mitral neurons, may provide valuable information. The expression of TH in these mutants is, by contrast with peripheral denervation, unaltered as compared with normal heterozygous littermates (Baker and Greer, 1990). Odor-induced activity and total peripheral innervation, but not deprivation of mitral cells, affect the TH-positive subpopulation of PG. The present work demonstrates that specific divergences in the olfactory receptor neuron synapses do not affect the distribution pattern of NOS in the mouse OB. It will be important to know whether other synaptic disruptions alter the expression of this enzyme, as it occurs for other transmitter systems.

ACKNOWLEDGMENTS

We thank Dr. Emson and Dr. Charles (Cambridge, UK) for the generous gift of the NOS antiserum. This work was supported by Junta de Castilla y León and DGICyT (PB94–1388) projects.

REFERENCES

Alonso JR, Sánchez F, Arévalo R, Carretero J, Aijón J, Vázquez R (1992): CaBP D-28k and NADPH-diaphorase coexistence in the magnocellular neurosecretory nuclei. Neuroreport 3:249–252.

Alonso JR, Arévalo R, Porteros A, Briñón JG, Lara J, Aijón J (1993): Calbindin D-28K and NADPH-diaphorase activity are localized in different populations of periglomerular cells in the rat olfactory bulb. J Chem Neuroanat 6:1–6.

Alonso JR, Arévalo R, Briñón JG, García-Ojeda E, Porteros A, Aijón J (1995a): NADPH-diaphorase staining in the central nervous system. In Wouterlood FG (ed): ''Neuroscience Protocols 050–04.'' Amsterdam: Elsevier, pp 1–11.

Alonso JR, Arévalo R, García-Ojeda E, Porteros A, Briñón JG, Aijón J (1995b): NADPH-diaphorase active and calbindin D-28k-immunoreactive neurons and fibers in the olfactory bulb of the hedgehog (*Erinaceus europaeus*). J Comp Neurol 351:307–327.

Alonso JR, Porteros A, García-Ojeda E, Bravo IG, Crespo C, Arévalo R, Aijón J (1996): Actividad NADPH-diaforasa (sintasa del óxido nítrico) en el bulbo olfatorio del mono macaco. In Suárez-Araujo CP, Regidor-García J (eds): ''Neurociencia y Computación Neuronal.'' Las Palmas de Gran Canaria, Spain: Ed. U.L.P.G.C., pp 73–80.

Baker H (1988): Neurotransmitter plasticity in the juxtaglomerular cells of the olfactory bulb. In Margolis FL, Getchell TV (eds): ''Molecular Neurobiology of the Olfactory System'' New York: Plenum Press, pp 185–216.

Baker H, Greer CA (1990): Region-specific consequences of PCD gene expression in the olfactory system. J Comp Neurol 293:125–133.

Baker H, Joh TH, Reis DJ (1980): Genetic control of the number of midbrain dopaminergic neurons in inbred strains of mice: Relationship to size and neuronal density of the striatum. Proc Natl Acad Sci USA 77:4369–4373.

Baker H, Joh TH, Ruggiero DA, Reis DJ (1983a): Variations in the number of dopamine neurons and tyrosine hydroxilase activity in hypothalamus of two mouse strains. J Neurosci 3:832–843.

Baker H, Kawano T, Margolis FL, Joh TH (1983b): Transneuronal regulation of tyrosine hydroxylase expression in olfactory bulb of mouse and rat. J Neurosci 3:69–78.

Baker H, Kawano T, Albert V, Joh TH, Reis DJ, Margolis FL (1984): Olfactory bulb dopamine neurons survive deafferentation-induced loss of tyrosine hydroxylase. Neuroscience 11:605–615.

Baker H, Morel K, Stone DM, Maruniak JA (1993): Adult naris closure profoundly reduces tyrosine hydroxylase expression in mouse olfactory bulb. Brain Res 614:109–116.

Bredt DS, Snyder SH (1992): Nitric oxide, a novel neuronal messenger. Neuron 8:3–11.

Bredt DS, Glatt CE, Hwang PM, Fotuhi M, Dawson TM, Snyder SH (1991a): Nitric oxide synthase protein and mRNA are discretely localized in neuronal populations of the mammalian CNS together with NADPH-diaphorase. Neuron 7:615–624.

Bredt DS, Hwang PM, Glatt CE, Lowenstein C, Reed RR, Snyder SH (1991b): Cloned and expressed nitric oxide synthase structurally resembles cytochrome P-450 reductase. Nature 351:714–718.

Breer H, Shepherd GM (1993): Implications of the NO/cGMP system for olfaction. Trends Neurosci 16:5–9.

Buwalda B, Nyakas C, Gast J, Luiten PGM, Schmidt HHHW (1995): Aldehyde fixation differentially affects distribution of diaphorase activity but not of nitric oxide synthase immunoreactivity in rat brain. Brain Res Bull 38:467–473.

Crespo C, Porteros A, Arévalo R, Briñón JG, Aijón J, Alonso JR (1996): Segregated distribution of nitric oxide synthase-positive cells in the periglomerular region of typical and atypical olfactory glomeruli. Neurosci Lett 205:149–152.

Croul-Ottman CE, Brunjes PC (1988): NADPH-diaphorase staining within the developing olfactory bulbs of normal and unilaterally odor-deprived rats. Brain Res 460:323–328.

Davis BJ (1991): NADPH-diaphorase activity in the olfactory system of the hamster and rat. J Comp Neurol 314:493–511.

Dawson VL (1995): Nitric oxide: Role in neurotoxicity. Clin Exp Pharmacol Physiol 22:305–308.

DellaCorte C, Kalinoski DL, Huque T, Wysocki L, Restrepo D (1995): NADPH diaphorase staining suggests localization of nitric oxide synthase within mature vertebrate olfactory neurons. Neuroscience 66:215–225.

Dryer L, Graziadei PP (1994): Influence of the olfactory organ on brain development. Perspect Dev Neurobiol 2:163–174.

Ehrlich ME, Grillo M, Joh TH, Margolis FL, Baker H (1990): Transneuronal regulation of neuronal specific gene expression in the mouse olfactory bulb. Mol Brain Res 7:115–122.

Epstein HT, Kaufman M, Saperstein A, Frank D, Huang S (1991): Strain differences in mouse brain weight gain and spatial-location scores during postnatal development. Biol Neonate 59:171–180.

Förstermann U, Kleinert H (1995): Nitric oxide synthase: Expression and expressional control of the three isoforms. Naunyn-Schmiedeberg's Arch Pharmacol 352:351–364.

Gabbott PLA, Bacon SJ (1996): Localisation of NADPH diaphorase activity and NOS immunoreactivity in astroglia in normal adult rat brain. Brain Res 714:135–144.

Halász N (1990): The vertebrate olfactory system. Chemical neuroanatomy, function and development. Budapest, Akadémiai Kiadó.

Herbison AE, Simonian SX, Norris PJ, Emson PC (1996): Relationship of neuronal nitric oxide synthase immunoreactivity to GnRH neurons in the ovariectomized and intact female rat. J Neuroendocrinol 8:73–82.

Hirsch DB, Steiner JP, Dawson TM, Mammen A, Hayek E, Snyder SH (1993): Neurotransmitter release regulated by nitric oxide in PC-12 cells and brain synaptosomes. Curr Biol 3:749–754.

Hope BT, Michael GJ, Knigge KM, Vincent SR (1991): Neuronal NADPH-diaphorase is a nitric oxide synthase. Proc Natl Acad Sci USA 88:2811–2814.

Jaffrey SR, Snyder SH (1995): Nitric oxide: A neural messenger. Annu Rev Cell Dev Biol 11:417–440.

Johnson MD, Ma PM (1993): Localization of NADPH-diaphorase activity in monoaminergic neurons of the rat brain. J Comp Neurol 332:391–406.

Key B, Akeson RA (1991): Delineation of olfactory pathways in the frog nervous system by unique glycoconjugates and N-CAM glycoforms. Neuron 6:381–396.

Kishimoto J, Keverne EB, Hardwick J, Emson PC (1993): Localization of nitric oxide synthase in the mouse olfactory and vomeronasal system: A histochemical, immunological and *in situ* hybridization study. Eur J Neurosci 5:1684–1694.

Knowles RG, Moncada S (1994): Nitric oxide synthases in mammals. Biochem J 298:249–258.

Kugler P, Drenckhahn D (1996): Astrocytes and Bergmann glia as an important site of nitric oxide synthase I. Glia 16:165–173.

Kulkarni AP, Getchell TV, Getchell ML (1994): Neuronal nitric oxide synthase is localized in extrinsic nerves regulating perireceptor processes in the chemosensory nasal mucosae of rats and humans. J Comp Neurol 345:125–138.

Le Jeune H, Jourdan F (1991): Postnatal development of cholinergic markers in the rat olfactory bulb: A histochemical and immunocytochemical study. J Comp Neurol 314:383–395.

Le Jeune H, Jourdan F (1993): Cholinergic innervation of olfactory glomeruli in the rat: An ultrastructural immunocytochemical study. J Comp Neurol 336:279–292.

Lewin B (1994): On neuronal specificity and the molecular basis of perception. Cell 79:935–943.

Macrides F, Davis FJ (1983): The olfactory bulb. In Emson PC (ed): ''Chemical Neuroanatomy.'' New York: Raven Press, pp 391–426.

Matsumoto T, Pollock JS, Nakane M, Förstermann U (1993): Developmental changes of cytosolic and particulate nitric oxide synthase in rat brain. Dev Brain Res 73:199–203.

Meisami E, Hamedi S (1986): Relative contribution of brain and peripheral connections to postnatal growth and cell accretion in the rat olfactory bulb. Brain Res 394:282–286.

Mori K (1987): Monoclonal antibodies (2C5 and 4C9) against lactoseries carbohydrates identify subsets of olfactory and vomeronasal receptor cells and their axons in the rabbit. Brain Res 408:215–221.

Nadi NS, Head R, Grillo M, Hempstead J, Grannot-Reisfeld N, Margolis FL (1981): Chemical deafferentation of the olfactory bulb: Plasticity of the levels of tyrosine hydroxylase, dopamine and norepinephrine. Brain Res 213:365–377.

Porteros A, Arévalo R, Crespo C, Briñón JG, Weruaga E, Aijón J, Alonso JR (1996): Nitric oxide synthase activity in the olfactory bulb of anuran and urodele amphibians. Brain Res 724:67–72.

Roskams AJ, Bredt DS, Dawson TM, Ronnett GV (1994): Nitric oxide mediates the formation of synaptic connections in developing and regenerating olfactory receptor neurons. Neuron 13:289–299.

Royet JP, Souchier C, Jourdan F, Ploye H (1988) Morphometric study of the glomerular population in the mouse olfactory bulb: Numerical density and size distribution along the rostrocaudal axis. J Comp Neurol 270:559–568.

Scherer-Singler U, Vincent SR, Dawson TM, Ronnett GV (1983) Demonstration of a unique population of neurons with NADPH-diaphorase histochemistry. J Neurosci Meth 9:229–234.

Schwarting GA, Crandall JE (1991): Subsets of olfactory and vomeronasal sensory epithelial cells and axons revealed by monoclonal antibodies to carbohydrate antigens. Brain Res 547:239–248.

Schwarting GA, Deutsch G, Gattey DM, Crandall JE (1992): Glycoconjugates are stage- and position-specific cell surface molecules in the developing olfactory system, 2: Unique carbohydrate antigens are topographic markers for selective projection patterns of olfactory axons. J Neurobiol 23:130–142.

Scott JW, McDonald JK, Pemberton JL (1987) Short-axon cells of the rat olfactory bulb display NADPH-diaphorase activity, neuropeptide Y-like immunoreactivity, and somatostatin-like immunoreactivity. J Comp Neurol 260:378–391.

Shepherd GM (1994): Discrimination of molecular signals by the olfactory receptor neurons. Neuron 13:771–790.

Solodkin A, Traub RJ, Gebhart GF (1992): Unilateral hindpaw inflammation produces a bilateral increase in NADPH-diaphorase histochemical staining in the rat lumbar spinal cord. Neuroscience 51:495–499.

Thomas E, Pearse AGE (1961): The fine localization of dehydrogenases in the nervous system. Histochemie 2:266–282.

Verge VMK, Xu Z, Xu X-J, Wiesenfeld-Hallin Z, Hökfelt T (1992): Marked increase in nitric oxide synthase mRNA in rat dorsal root ganglia after peripheral axotomy: *In situ* hybridization and functional studies. Proc Natl Acad Sci USA 89:11617–11621.

Vincent SR, Kimura H (1992): Histochemical mapping of nitric oxide synthase in the rat brain. Neuroscience 46:755–784.

Vizzard MA, Erdman SL, de Groat WC (1993): The effect of rhizotomy on NADPH-diaphorase staining in the lumbar spinal cord of the rat. Brain Res 607:349–353.

White EL (1972): Synaptic organization in the olfactory glomerulus of the mouse. Brain Res 37:69–80.

White EL (1973): Synaptic organization of the mammalian olfactory glomerulus: New findings including an intraspecific variation. Brain Res 60:299–313.

Wolf G (1997): Nitric oxide and nitric oxide synthase: Biology, pathology, localization. Histol Histopathol 12:251–261.

Wu W (1993): Expression of nitric-oxide synthase (NOS) in injured CNS neurons as shown by NADPH-diaphorase histochemistry. Exp Neurol 120:153–159.

Zheng LM, Jourdan F (1988): Atypical olfactory glomeruli contain original olfactory axon terminals: An ultrastructural horseradish peroxidase study in the rat. Neuroscience 26:367–378.